Vortex slush regime in the Josephson vortex phase diagram of 60-K $YBa_2Cu_3O_{7-\delta}$ single crystals

Tomoyuki Naito,[1,*] Hideo Iwasaki,[1] Terukazu Nishizaki,[2] Seiya Haraguchi,[1] Yuuya Kawabata,[1] Kenji Shibata,[2] and Norio Kobayashi[2]

[1]*School of Materials Science, Japan Advanced Institute of Science and Technology (JAIST), Tatsunokuchi 923-1292, Japan*

[2]*Institute for Materials Research, Tohoku University, Sendai 980-8577, Japan*

(Received 7 December 2002; revised manuscript received 24 July 2003; published 29 December 2003)

We have studied the Josephson vortex phase diagram of 60-K $YBa_2Cu_3O_{7-\delta}$ single crystals by measuring the in-plane resistivity. We find that the phase transition of the Josephson vortices in high magnetic fields above 60 kOe is a two-stage process which consists of first-order vortex liquid-to-slush and second-order vortex slush-to-glass transitions, while a single second-order vortex liquid-to-glass transition is observed in low magnetic fields below 50 kOe. The obtained results show that the vortex slush appears as the intermediate regime between the ordinary vortex liquid and glassy phases in the Josephson vortex system.

DOI: 10.1103/PhysRevB.68.224516 PACS number(s): 74.25.Qt, 74.25.Fy, 74.72.Bk

I. INTRODUCTION

In the mixed state of high-temperature superconductors, the vortex phase diagram for a magnetic field applied parallel to the ab plane ($H\|ab$) is still unclear, in contrast to that for the $H\|c$ axis. For $H\|ab$, since the so-called Josephson vortices (JV's) are formed between the neighboring superconducting layers, their phase transition is significantly affected by the layered structure. In the 90-K phase of $YBa_2Cu_3O_{7-\delta}$ (YBCO) single crystals, the in-plane resistivity experiments by Kwok *et al.*[1] showed that a first-order transition is suppressed by intrinsic pinning[2] and the possibility of a transition between the vortex smectic and liquid phases on the analogy of that between the nematic and smectic-*A* phases in liquid crystals.[3] Later, motivated by Ref. 1, Balents and Nelson[4] theoretically revealed that the second-order vortex liquid-to-smectic transition occurs between the liquid and solid phases and predicted the complex behavior of this transition line as a result of the commensurability effect of the vortex density with the interlayer distance. Experiments in 90-K YBCO by Grigera *et al.*[5] and results of a computer simulation by Laguna *et al.*[6] supported this scenario by observing a two-step transition.

In oxygen deficient YBCO single crystals, Gordeev *et al.*[7] observed a vertical and oscillating melting line characterized by a jump in the in-plane resistivity and attributed it to the appearance of the smectic phase. It seems that there is a resistive tail below the jump; however, they did not discuss the lower transition between the smectic and solid phases. Lundqvist *et al.* also reported similar vertical transition lines for such materials from both the in-plane[8] and out-of-plane[9] resistivity measurements. Only a single resistive transition was found in both results, demonstrating the absence of an intermediate region like the smectic phase. On the other hand, the vortex slush regime, which was reported by Worthington *et al.*[10] for $H\|c$ in proton irradiated 90-K YBCO, is well known as an intermediate phase between vortex liquid and vortex glass. In Ref. 10, the authors found a two-stage transition comprised of discontinuous and continuous behaviors and interpreted it as follows: upon cooling the liquid undergoes a first-order transition into slush, and the slush freezes into the vortex glass phase via a second-order transition. For $H\|ab$, such a regime has not been experimentally observed, but was theoretically confirmed by Ikeda.[11] Consequently, in oxygen deficient YBCO, although several experimental observations which indicate transitions of the JV's have been reported, the nature of those transitions seems not to be settled.

In this paper, we report the JV phase diagram in 60-K YBCO single crystals. We find a two-stage resistive transition consisting of both the jump and continuous behaviors in high magnetic fields above 60 kOe and show that the two transitions consist of first-order liquid-to-slush and second-order slush-to-glass. On the other hand, the liquid directly freezes into glass via a second-order transition in low magnetic fields below 50 kOe. Our findings are evidence that the vortex slush regime exists in the JV phase diagram.

II. EXPERIMENT

YBCO single crystals were grown by a self-flux method in yttria crucibles.[12] Twinned 60-K phase crystals were obtained by annealing at 680 °C for 1 week in 1 bar flowing oxygen gas, followed by quenching in liquid nitrogen. The superconducting transition temperature T_c defined at the zero resistivity is 62.4 K. The sample dimensions are $0.8\times0.6\times0.2$ mm^3. The in-plane resistivity ρ is measured by a conventional dc four-probe method with a typical current density J of 0.6 A/cm^2 in magnetic fields up to 150 kOe. The sample position is adjusted with the angle resolution of $\sim0.01°$, where the angle ϕ is defined between the magnetic-field direction and the ab plane; the current direction is always perpendicular to the former. The experimental configuration is schematically illustrated in the inset of Fig. 1. The anisotropic parameter $\gamma(=\xi_{ab}/\xi_c)$ of the crystal is determined to be ~17 from scaling the set of the $\rho(\phi)$ curves measured in several magnetic fields up to 90 kOe by the reduced field, $H_{\rm red}=H(\sin^2\phi+\gamma^{-2}\cos^2\phi)^{1/2}$, based on the effective mass model,[13] where ξ_{ab} and ξ_c are the coherence length in the ab plane and along the c axis direction, respectively.

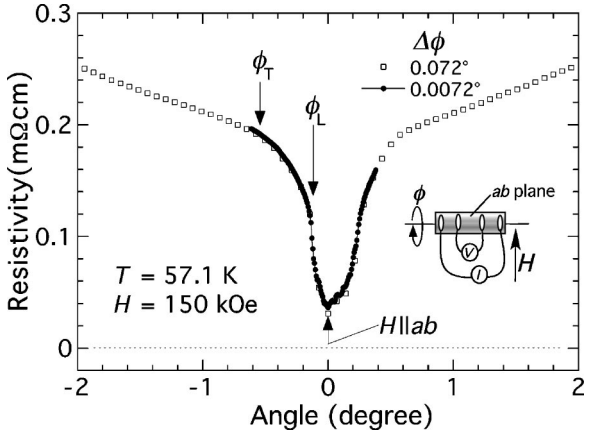

FIG. 1. Angular dependence of the resistivity $\rho(\phi)$ at $T=57.1$ K and $H=150$ kOe near $H\|ab$, where the angle ϕ is defined between the magnetic field and ab plane. The specific angles ϕ_T and ϕ_L represent the so-called trapping and lock-in angles, respectively. A schematic picture of the experimental configuration is shown in the inset; the current direction is always perpendicular to the magnetic-field direction.

III. RESULTS

Figure 1 shows the angular dependence of the resistivity $\rho(\phi)$ at $H=150$ kOe and $T=57.1$ K near $H\|ab$. The angle at the resistivity minimum indicating $H\|ab$ is defined as $\phi=0°$. The resistivity linearly depends on ϕ at high angles. Below a certain angle, indicated as $|\phi_T|\sim 0.6°$, the resistivity starts to deviate from its linear behavior and rapidly decreases, indicating that the vortices begin to be confined between the layers. A sharp dip appears below $|\phi_L|\sim 0.15°$, demonstrating the lock-in transition. The specific angles ϕ_L and ϕ_T are the so-called lock-in and trapping angles, respectively.

Figure 2 shows the temperature dependence of the resistivity $\rho(T)$ at $\phi=0°$ in several magnetic fields up to 150 kOe. In high magnetic fields above 60 kOe, the $\rho(T)$ curves represent a two-stage transition; upon cooling, they first show a somewhat sharp jump toward nonzero resistivity and next a gradual temperature dependence accompanied by a continuous transition. On the other hand, in low magnetic fields below 50 kOe, the $\rho(T)$ curves show only a continuous transition. The inset of Fig. 2 demonstrates the $\rho(T)$ curves for several current densities of 0.6, 1.2, and 2.0 A/cm^2 at 130 kOe. In the low-resistivity regime below 10^{-3} mΩ cm, one can find a slight nonlinear (non-Ohmic) behavior among the curves. However, this feature is caused by only the $\rho(T)$ curve at 2.0 A/cm^2. Futhermore, the other curves for 0.6 and 1.2 A/cm^2, show a similar temperature dependence. Thus we consider that the current density of 0.6 A/cm^2 typically used here gives a linear (Ohmic) resistivity.

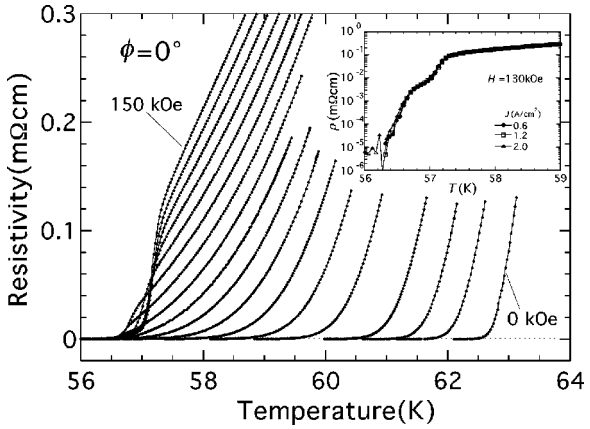

FIG. 2. Temperature dependence of the resistivity for $\phi=0°$ ($H\|ab$) in several magnetic fields of 0, 2, 5, and from 10 to 150 kOe in intervals of 10 kOe. Inset shows the $\rho(T)$ curves for several current densities of 0.6, 1.2, and 2.0 A/cm^2 at $H=130$ kOe.

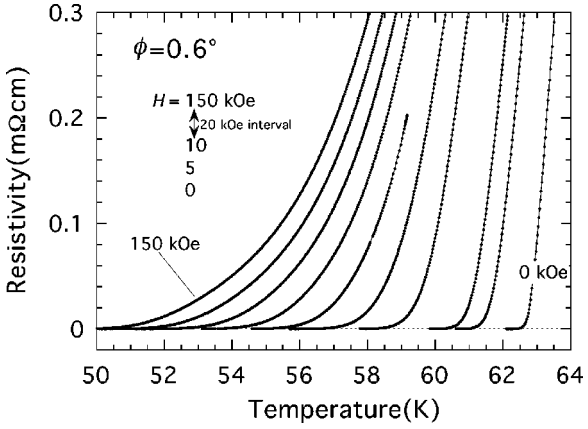

FIG. 3. Temperature dependence of the resistivity for $\phi=0.6°$ in several magnetic fields up to 150 kOe.

Figure 3 shows the temperature dependence of the resistivity for $\phi=0.6°$, just above the trapping angle, in magnetic fields up to 150 kOe. The anomalous feature as observed for $\phi=0°$ completely disappears, and only a continuous transition occurs.

The discontinuous transition temperature for $\phi=0°$ in high magnetic fields is defined as the temperature at which

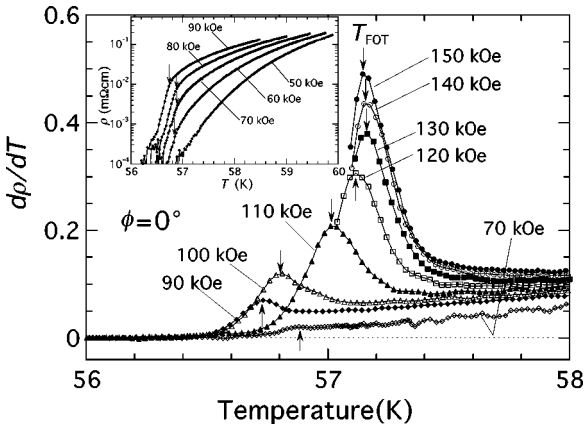

FIG. 4. The main panel shows the resistivity-temperature derivative $d\rho/dT$ versus T plot for $\phi=0°$ in several magnetic fields above 70 kOe. The first-order transition temperature T_{FOT}, indicated by the arrow, is defined at the peak temperature. The inset shows the $\rho(T)$ curves at 50, 60, 70, 80, and 90 kOe; the arrows here also indicate T_{FOT}.

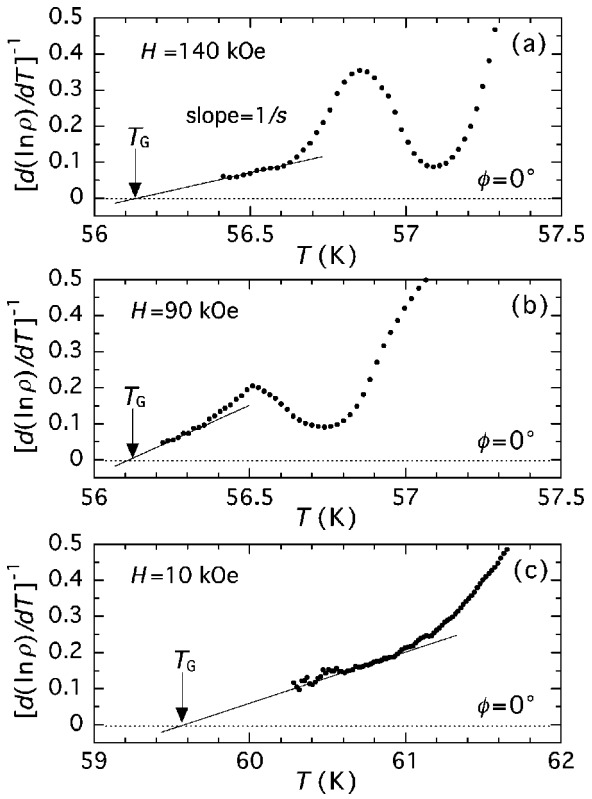

FIG. 5. The $[d(\ln\rho)/dT]^{-1}$ versus T plots near the liquid-to-glass transition temperature T_G at $\phi=0°$ for several magnetic fields; (a) $H=140$ kOe, (b) 90 kOe, and (c) 10 kOe.

the temperature derivative of the resistivity $d\rho/dT$ becomes a maximum, as shown in Fig. 4. The jump width tends to sharpen with increasing magnetic field and becomes the narrowest at 150 kOe. Below 80 kOe, the $d\rho/dT$ peak is obscure; however, the discontinuous feature seems to still survive down to 60 kOe, as seen in the inset of Fig. 4. Although resistivity is not a thermodynamic quantity, its jump is observed at the well-defined first-order melting transition probed by the thermodynamic measurements.[14] Furthermore, Nishizaki *et al.*[15] found a similar two-stage resistive transition for $H\|c$ in optimally doped YBCO and confirmed that the incomplete resistivity jump is attributed to the first-order transition, based on the observation of the magnetization jump at the same point. Therefore we regard the discontinuous transition observed here as first order and denote the transition temperature as T_{FOT}.

The continuous transition means that the vortex phase transition is second-order vortex liquid-to-glass; several glass phases,[16,17] which depend on the type of dominant pinning center, are possible. The theories[11,16,17] describing such a transition give the relation of the linear resistivity to the temperature in the critical region as follows: $\rho(T)\propto(T-T_G)^s$. This was originally proposed by Fisher *et al.*[16] in the vortex glass theory, where T_G is a glass transition temperature and s is a critical exponent. The details of s vary with the type of glass phase, for instance, s is $\nu(z-d+2)$ in Ref. 16, where z and ν, respectively, are the dynamic and static exponents and d is the system dimension. As already confirmed in the inset of Fig. 2, the resistivity data obtained here belong

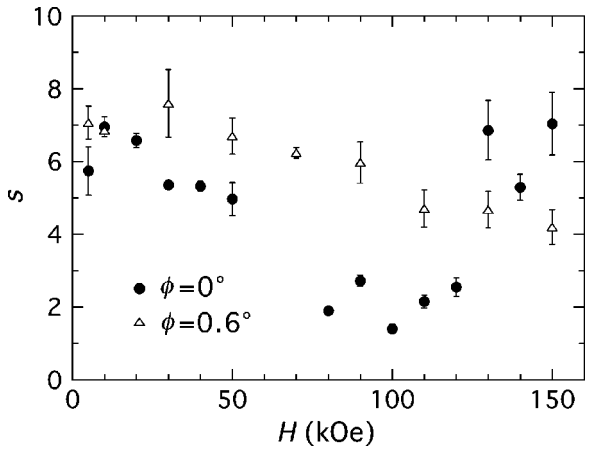

FIG. 6. Magnetic-field dependence of the critical exponent s for both $\phi=0°$ (closed circles) and 0.6° (open triangles).

to the linear regime. Using this relation therefore we estimated the T_G and s values from a straight line extrapolation to the temperature axis and the inverse of the slope in the $[d(\ln\rho)/dT]^{-1}$ vs T plot, respectively, regardless of the glass types. Typical data for $\phi=0°$ are shown in Figs. 5(a)–5(c). As seen in Figs. 5(a) and 5(b), in the intermediate and high magnetic fields, the linear part of the plot which represents the critical region is quite narrow. However, it seems that this does not affect the determination of the T_G value. Actually, the T_G values are determined with very small uncertainly; for instance, the obtained T_G values for $H=140$ and 90 kOe are of 56.13 ± 0.04 K and 56.10 ± 0.02 K, respectively. On the other hand, the critical region is relatively wide in the low magnetic fields; at $H=10$ kOe the obtained T_G value is of 59.58 ± 0.02 K, as demonstrated in Fig. 5(c). We note that the T_G for $H=60$ and 70 kOe cannot be estimated in our experimental window. This seems to be caused by the fact that the very small difference between the T_{FOT} and the temperature at the zero-resistiviy transition smears out the critical region;

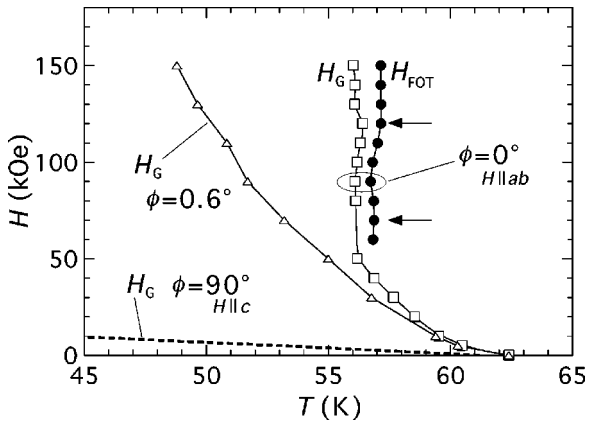

FIG. 7. Magnetic field versus temperature phase diagram. The closed circles represent the first-order transition line for $\phi=0°$. The arrows indicate the commensurate field. The open squares represent the second-order liquid-to-glass transition line for $\phi=0°$. The open triangles and thin broken line represent the vortex glass transition line for $\phi=0.6°$ and 90° ($H\|c$) (Ref. 18), respectively.

thus, we do not discard the occurrence of the second-order liquid-to-glass transition there. Figure 6 shows the magnetic field dependence of s for both $\phi=0°$ and 0.6°. The former is classified into three distinct regions; we will try to explain this nonuniversal behavior later. On the other hand, the latter monotonically decreases with increasing magnetic field.

Figure 7 shows the magnetic field versus temperature phase diagram of 60-K YBCO near $H\|ab$; $H_{\mathrm{FOT}}(T)$ and $H_{\mathrm{G}}(T)$ correspond to $T_{\mathrm{FOT}}(H)$ and $T_{\mathrm{G}}(H)$, respectively. The first-order transition line $H_{\mathrm{FOT}}(T)$ for $\phi=0°$ is almost independent of the temperature and obviously oscillates between $60\leqslant H\leqslant 120$ kOe. This line suddenly appears at around 60 kOe and survives up to the highest magnetic field achieved in our facilities, therefore we can recognize that the lower critical point $H_{\mathrm{FOT}}^{\mathrm{lcp}}$ exists at or below 60 kOe, but we do not know where the upper one $H_{\mathrm{FOT}}^{\mathrm{ucp}}$ is located. The second-order transition line $H_{\mathrm{G}}(T)$ for $\phi=0°$ below 50 kOe monotonically depends on temperature with the empirical power-law dependence as $\propto(1-T/T_c)^{1.7}$, which has behavior similar to that for $H\|c$.[18] However, it is also vertical above 50 kOe and oscillates between $80\leqslant H\leqslant 130$ kOe. Above 130 kOe, it begins to deviate from the $H_{\mathrm{FOT}}(T)$ line without the oscillation. One can easily find the intermediate region between the $H_{\mathrm{FOT}}(T)$ and $H_{\mathrm{G}}(T)$ lines. For $\phi=0.6°$, on the other hand, the obtained $H_{\mathrm{G}}(T)$ line shows a monotonic power-law dependence as $\propto(1-T/T_c)^{1.9}$ without the vertical and oscillating behaviors, strongly indicating that such anomalous features are truly intrinsic phenomena of the JV system.

IV. DISCUSSION

A. Nature of the first-order transition for $\phi=0°$

As seen in the $H-T$ phase diagram, although the lower critical point $H_{\mathrm{FOT}}^{\mathrm{lcp}}$ is obviously in the liquid region, the upper one $H_{\mathrm{FOT}}^{\mathrm{ucp}}$ is beyond our experimental window. To clarify the nature of the first-order transition, we first examined whether $H_{\mathrm{FOT}}^{\mathrm{ucp}}$ exists in finite temperature. The flexibility of the JV's configuration along the c axis tends to decrease with increasing magnetic field due to the layered structure of the crystal, giving rise to the fact that the configuration is dominated by the interaction of the JV's in the same layer. Such an effect prevents the JV's from constructing a lattice, i.e., the first-order transition tends to be suppressed with increasing magnetic field. This picture is supported by the results of the Monte Carlo simulation performed by Hu and Tachiki[19] who found the critical point of the phase transition in the JV system at a certain magnetic field given as $\phi_0/2\sqrt{3}\gamma l^2$, where ϕ_0 is the flux quantum and l is the interlayer spacing. In 60-K YBCO, the first-order phase transition is expected to disappear at around 253 kOe using this relation with the values of $\gamma=17$ and $l=11.8$ Å. Furthermore, the upper critical end point of the first-order transition line was found in the JV phase diagram theoretically achieved in Ref. 11. Therefore it becomes clear that the $H_{\mathrm{FOT}}(T)$ line is in the liquid region, meaning that the two kinds of liquids must exist above and below it.

The incomplete resistivity jump strongly indicates that positional short-range ordered JV's exist below the line, because the resistivity should jump to the zero resistivity if the positional order is long range, as observed at the first-order melting transition for $H\|c$.[14] Worthington *et al.*[10] previously found a similar two-stage resistive behavior for $H\|c$ in proton-irradiated 90-K YBCO and introduced the concept of vortex slush to explain the intermediate regime between the two transitions; the validity of this idea has been confirmed by a number of studies which include experiments,[15] theories,[11,20] and Monte Carlo simulation.[21] In this regime, the vortices are thought to have a short-range translational order but no long-range phase order,[10] i.e., the vortex slush is a kind of vortex liquid; thus, this picture is in good agreement with the fact that the $H_{\mathrm{FOT}}(T)$ line lies in the liquid regime. Moreover, in both reported experiments,[10,15] the lower temperature region below the gradual transition is the vortex glass phase, which also significantly resembles our results. Although the previous reports[10,15,20,21] were mostly about the configuration for $H\|c$, Ikeda recently theoretically predicted that the vortex slush regime also appears for $H\|ab$,[11] which strongly supports our results.

One can notice that the oscillating $H_{\mathrm{FOT}}(T)$ line relates to the commensurability between a period of the JV's configuration and the interlayer spacing. Ikeda and Isotani[22] actually predicted an oscillating first-order melting transition line in the disorder-free JV system as a result of the fact that a successive structural phase transition[23] occurs as a function of the magnetic field. They predicted that such a sequence of the structural transitions would be found between the commensurate and incommensurate lattices. Since the melting temperature T_{m} is determined by the robustness of the lattice against the thermal fluctuation, the former T_{m} is expected to be higher than the latter one, resulting in oscillation of the melting line. In this study therefore it seems that the commensurate lattice appears at around 70 and 120 kOe, as expressed by arrows in Fig. 7. According to Ref. 22, two types of commensurate states appear. One is an ordinary lattice defined by the integer w, which describes the ratio between the period of a lattice and the interlayer spacing [i.e., the $(w-1)l$ layers exist between the layers occupied by the JV's]; e.g., in a $w=1$ lattice, a vacant layer without vortices is absent. Such an *integer* lattice is naturally expected to be strongly pinned by intrinsic pinning, because each vortex exists just in the middle of the adjacent layers. A lattice with a fraction w is also possible, where an integer lattice and an unpinned lattice, which is composed of the vortices located not in the middle of the neighboring layers, coexist; however, such a *fractional* lattice is easily destroyed by the disorders in the crystals. Thus it is adequate here that we consider integer lattices. The commensurability condition[22] of the integer lattice is theoretically given as $pw^2/\pi=\sqrt{3}$ or $1/\sqrt{3}$, where $p(=2\pi l^2\gamma H/\phi_0)$ is the dimensionless magnetic field. Using values of $\gamma=17$ and $l=11.8$ Å, this relation with $w=2$ and 3 gives a commensurate field of 63 and 84 kOe, respectively, so that these obtained values can explain one of the commensurate magnetic fields at around 70 kOe. On the other hand, we cannot find any commensurate integer lattice at around 120 kOe. Recently, Ikeda[24] precisely re-examined the structure of the JV lattice at around $p\simeq 1$ and considered the special $w=1$ lattices which are created by rotating the

basis vectors $\boldsymbol{a}_1$ and $\boldsymbol{a}_2$ of the ordinary integer lattices counter-clockwise by an angle θ in the ac plane. Here, the component of the c-axis direction of the rotated basis vectors $a_1^c(\theta)$ and $a_2^c(\theta)$ must satisfy the following condition: $Ma_1^c(\theta)=Na_2^c(\theta)=MNl$, where M and N are positive integers. Such rotated lattices were named (M,N) lattices; their commensurability condition[24] is given as $p=\sqrt{3}\pi/(M^2+N^2-MN)$. According to the computed results in Ref. 24, the commensurate field of the (3, 1) state is 107 kOe, and this structure is stable in the wide field range between 101 and 134 kOe, therefore the commensurate field at around 120 kOe seems to come from the appearance of the (3, 1) lattice. The oscillating behavior above 120 kOe is obscure in comparison with that below 110 kOe, because commensurability effects have a tendency to disappear as the flexibility of the JV configuration along the c axis direction diminishes.

A similar vertical and oscillating transition line defined by the resistivity jump was previously reported by Gordeev *et al.* in oxygen deficient YBCO.[7] They interpreted that the latter feature comes from the appearance of the vortex smectic phase, because the vortex liquid-to-smectic transition line was predicted to oscillate as a result of the commensurability effect by Balents and Nelson theoretically.[4] According to Ref. 4, the vortices in the smectic phase have a positional ordering along the c axis but not one in the ab planes, just like an ordinary liquid; i.e., the vortex smectic phase is also a kind of liquid. Although this picture seems to explain our results, we cannot accept it for the following reason. The authors of Ref. 4 predicted that the liquid-to-smectic transition is second-order, which is evidently contradicted by the nature of the resistivity jump found here.

Recently, in oxygen deficient YBCO single crystals with $T_c=59.6$ and 60.6 K, Lundqvist *et al.*[9] found the single vertical transition line characterized by a sharp drop in the out-of-plane resistivity. Although they did not describe the detailed nature of the JV transition, as mentioned above, such a complete resistivity drop means that the liquid phase freezes not into slush, but into lattice, via the first-order transition upon cooling. On the other hand, they also obtained nearly field-independent liquid-to-glass transition lines from the in-plane resistivity measurements[8] in several oxygen deficient YBCO single crystals which are not the identical samples of Ref. 9. It is well known that the first-order transition of vortices can be observed in clean crystals and that it is destroyed by a pinning effect, which leaves us with a question about the quality of both our sample and theirs. However, both crystals have almost the same quality, judging from the superconducting transition width ΔT_c in the zero magnetic field; both transition widths are about 2 K. Let us now consider the difference between our results and those of Ref. 9 in terms of the experimental configuration. Under the $H\|ab$ and $I\|c$ condition, the Lorentz force F_L moves the JV's along the layer, so that the intrinsic pinning is not effective. On the other hand, it naturally becomes the most effective under a typical configuration of the in-plane resistivity measurement($H\perp I$). Therefore it seems valid that the anisotropy of the pinning strength induced by the F_L direction causes such a change in the vortex phase transition. Moreover, a similar phenomenon can be found in the vortex phase diagram of optimally doped YBCO for $H\|c$,[15] where the first-order vortex lattice melting transition in the low magnetic fields changes to the first-order liquid-to-slush transition in the high magnetic fields, which is thought to come from the increase in the effectiveness of the pinning disorder with increasing magnetic field. Next, we consider why the first-order transition was not detected in Ref. 8. In 90-K YBCO,[15,25] the slight increase of the amount of oxygen vacancy, which lowers the T_c but hardly affects the ΔT_c, easily destroys the first-order transition. Thus we speculate that the amount of pinning disorders, which do not explicitly contribute to the ΔT_c, but affects the vortex phase transition, in samples of Ref. 8 is greater than that in ours.

B. Nature of the second-order transition for $\phi=0°$

The oscillation of the $H_G(T)$ line seems to synchronize to that of the $H_{FOT}(T)$ line, meaning that the glass transition temperature also is elevated by the commensurability effect, i.e., the intrinsic pinning grows stronger. This picture is very similar to the Bose glass transition,[17] which has been observed for $H\|c$ in crystals with correlated disorders such as twin planes[26] and columnar defects;[27] the Bose glass transition temperature tends to increase when the pinning effect strengthens. The nonsuperconducting layers act as a correlated pinning center if the intrinsic pinning is effective, making the Bose glass phase possible; the small s values in this region also support this possibility (see next paragraph). Above 130 kOe, the $H_G(T)$ line does not oscillate and monotonically deviates from the $H_{FOT}(T)$ line, which represents the fact that the commensurability effect is almost negligible in high magnetic fields, as found for the $H_{FOT}(T)$ line in the same magnetic-field range.

We consider the nonuniversality of the critical exponent s, to clarify any doubt about the occurrence of the second-order liquid-to-glass transition. In the low magnetic fields below 50 kOe, the s value is 5.9 ± 1.4, which is consistent with the reported values of $s=6-8$ (Ref. 14) in the vortex glass transition. Therefore, in this region, the vortex glass transition undoubtedly occurs. The s value abruptly jumps to the smaller class of 1.3–2.9 between $80\leqslant H\leqslant120$ kOe. A similar small s value has been found in the Bose glass transition, for instance, $s=2.8\pm0.2$ in twinned 90-K YBCO,[26] $s=3.5\pm0.5$ in Bi-2212 with columnar defects,[27] and $s=2.6$ in the results of the Monte Carlo simulation.[28] Thus the small s value in the intermediate magnetic fields supports the Bose glass transition, as discussed in the preceding paragraph. In the high magnetic fields above 130 kOe, the s value belongs to the larger class of 5–8 again, therefore the glass phase is expected to be not Bose glass, but vortex glass. This is consistent with the fact that the commensurability effect is weak in this region. Consequently, we conclude that the continuous transition observed here represents that the vortex slush or liquid freezes into the glassy phase via a second-order transition upon cooling, even though the critical behavior is nonuniversal.

V. CONCLUSION

We have studied the Josephson vortex phase diagram on 60-K YBCO single crystals by measuring the in-plane resistivity. We found that a two-stage phase transition, consisting of a first-order liquid-to-slush and a second-order slush-to-glass transitions, occurs in high magnetic fields above 60 kOe, and that the single second-order liquid-to-glass transition occurs in low magnetic fields below 50 kOe. Our results demonstrate that the vortex slush regime exists as the intermediate phase between the glassy and the ordinary liquid phases in the Josephson vortex phase diagram.

ACKNOWLEDGMENTS

The authors would like to thank R. Ikeda and X. Hu for their helpful discussions, and H. Kita, H. Komatsu, I.Kimura, T. Horigome, and M. Uno for assisting with the experiments. We also would like to acknowledge J. A. Steeh for reviewing and editing this paper. The experiments were in part performed at the High Field Laboratory for Superconducting Materials, IMR, Tohoku University and at Low Temperature Science Division, Center for Low Temperature Science, Tohoku University. One of the authors (T.N.) was financially supported by a Grant for Basic Science Research Projects (Grant No. 000539) from the Sumitomo Foundation.

*Electronic address: tomon@jaist.ac.jp

[1] W. K. Kwok, J. Fendrich, U. Welp, S. Fleshler, J. Downey, and G. W. Crabtree, Phys. Rev. Lett. **72**, 1088 (1994).
[2] M. Tachiki and S. Takahashi, Solid State Commun. **70**, 291 (1989); **72**, 1083 (1989).
[3] P. G. de Gennes, Solid State Commun. **10**, 753 (1972).
[4] L. Balents and D. R. Nelson, Phys. Rev. Lett. **73**, 2618 (1994); Phys. Rev. B **52**, 12 951 (1995).
[5] S. A. Grigera, E. Morre, E. Osquiguil, G. Nieva, and F. de la Cruz, Phys. Rev. B **59**, 11 201 (1999).
[6] M. F. Laguna, D. Dominguez, and C. A. Balseiro, Phys. Rev. B **62**, 6692 (2000).
[7] S. N. Gordeev, A. A. Zhukov, P. A. J. de Groot, A. G. M. Jansen, R. Gagnon, and L. Taillefer, Phys. Rev. Lett. **85**, 4594 (2000).
[8] B. Lundqvist Ö. Rapp, and M. Andersson, Phys. Rev. B **62**, 3542 (2000).
[9] B. Lundqvist Ö. Rapp, M. Andersson, and Yu. Eltsev, Phys. Rev. B **64**, 060503 (2001).
[10] T. K. Worthington, M. P. A. Fisher, D. A. Huse, J. Toner, A. D. Marwick, T. Zabel, C. A. Feild, and F. Holtzberg, Phys. Rev. B **46**, 11 854 (1992).
[11] R. Ikeda and H. Adachi, J. Phys. Soc. Jpn. **69**, 2993 (2000).
[12] T. Naito, T. Nishizaki, Y. Watanabe, and N. Kobayashi, in *Advances in Superconductivity IX*, edited by S. Nakajima and M. Murakami (Springer-Verlag, Tokyo, 1997), p. 601.
[13] G. Blatter, V. B. Geshkenbein, and A. I. Larkin, Phys. Rev. Lett. **68**, 875 (1992).
[14] For a review, T. Nishizaki and N. Kobayashi, Supercond. Sci. Technol. **13**, 1 (2000), and references therein.
[15] T. Nishizaki, K. Shibata, T. Sasaki, and N. Kobayashi, Physica C **341–348**, 957 (2000); K. Shibata, T. Nishizaki, T. Sasaki, and N. Kobayashi, Phys. Rev. B **66**, 214518 (2002).
[16] M. P. A. Fisher, Phys. Rev. Lett. **62**, 1415 (1989); D. S. Fisher, M. P. A. Fisher, and D. A. Huse, Phys. Rev. B **43**, 130 (1991).
[17] D. R. Nelson and V. M. Vinokur, Phys. Rev. Lett. **68**, 2398 (1992); Phys. Rev. B **48**, 13 060 (1993).
[18] T. Naito, H. Iwasaki, T. Nishizaki, K. Shibata, and N. Kobayashi (unpublished).
[19] X. Hu and M. Tachiki, Phys. Rev. Lett. **85**, 2577 (2000).
[20] R. Ikeda, J. Phys. Soc. Jpn. **65**, 3998 (1996).
[21] Y. Nonomura and X. Hu, Phys. Rev. Lett. **86**, 5140 (2001).
[22] R. Ikeda and K. Isotani, J. Phys. Soc. Jpn. **68**, 599 (1999).
[23] L. Bulaevskii and J. R. Clem, Phys. Rev. B **44**, 10 234 (1991).
[24] R. Ikeda, J. Phys. Soc. Jpn. **71**, 587 (2002).
[25] A. I. Rykov, S. Tajima, F. V. Kusmartsev, E. M. Forgan, and Ch. Simon, Phys. Rev. B **60**, 7601 (1999).
[26] S. A. Grigera, E. Morre, E. Osquiguil, C. Balseiro, G. Nieva, and F. de la Cruz, Phys. Rev. Lett. **81**, 2348 (1998).
[27] W. S. Seow, R. A. Doyle, Y. Yan, A. M. Campbell, T. Mochiku, K. Kadowaki, and G. Wirth, in *Critical Currents in Superconductors*, edited by T. Matsushita and K. Yamafuji (World Scientific, Singapore, 1996), p. 149.
[28] J. Lidmar and M. Wallin, Europhys. Lett. **47**, 494 (1999).